



Intra- and Intertree Variability of the $^{87}\text{Sr}/^{86}\text{Sr}$ Ratio in Apple Orchards and Its Correlation with the Soil $^{87}\text{Sr}/^{86}\text{Sr}$ Ratio

Agnese Aguzzoni,^{*,†,‡,§} Michele Bassi,^{†,§} Peter Robatscher,[§] Francesca Scandellari,[‡] Werner Tirler,^{||} and Massimo Tagliavini[‡]

[‡]Free University of Bolzano, Piazza Università 1, 39100 Bolzano, Italy

[§]Laimburg Research Centre, 39040 Vadena, Italy

^{||}Eco-Research srl, Via Luigi Negrelli 13, 39100 Bolzano, Italy

Supporting Information

ABSTRACT: The $^{87}\text{Sr}/^{86}\text{Sr}$ ratio of horticultural products mostly derives from that of the bioavailable Sr fraction of the soil where they grow and, therefore, varies according to the local geolithological features. This study investigated the intra- and intertree variability of the $^{87}\text{Sr}/^{86}\text{Sr}$ ratio in two apple orchards in South Tyrol and its relation with the soil $^{87}\text{Sr}/^{86}\text{Sr}$ ratio. In both orchards, a moderate homogeneity of the $^{87}\text{Sr}/^{86}\text{Sr}$ ratio was observed among subsamples of the same tree part (shoot axes, leaves, apple peels, and pulps). Moreover, the $^{87}\text{Sr}/^{86}\text{Sr}$ ratio homogeneity among tree parts was high intratree and low intertree. The variability of the $^{87}\text{Sr}/^{86}\text{Sr}$ ratio within the tree and within the orchard is explained in light of the $^{87}\text{Sr}/^{86}\text{Sr}$ ratios of the soil. This $^{87}\text{Sr}/^{86}\text{Sr}$ variability within orchards does not preclude its use as a geographical tracer; however, this aspect should be evaluated to correctly design a sampling campaign or to generalize the results.

KEYWORDS: strontium isotopes, soil-derived marker, local fingerprint, *Malus × domestica* Borkh., MC ICP–MS

INTRODUCTION

The strontium isotope ($^{87}\text{Sr}/^{86}\text{Sr}$) ratio is a powerful marker used in traceability studies in several fields, including archeology and forensic, environmental, and food sciences. The use of this approach in horticulture has already allowed for a successful discrimination of produces according to their geographical origin.^{1–4} Hence, its analysis is considered a robust and suitable analytical technique helpful as an antifraud tool.⁵

Strontium has four stable natural isotopes, ^{84}Sr (0.56%), ^{86}Sr (9.86%), ^{87}Sr (7.0%), and ^{88}Sr (82.58%), and their relative composition is not constant but varies over a geological time scale as a result of the increase of the ^{87}Sr abundance. Indeed, ^{87}Sr is radiogenic, and its current abundance is the sum of the primordial ^{87}Sr and the radiogenic ^{87}Sr fraction coming from the radioactive decay of ^{87}Rb (half-life time = 48.8×10^9 years).⁶ The mineral Sr isotope composition varies according to the age of the mineral and its initial Rb/Sr ratio. Older rocks show a more radiogenic Sr composition compared to younger rocks, assuming they have the same initial Rb/Sr ratio. Within the same rock formation period, rocks with a higher initial Rb/Sr ratio reach higher values of the $^{87}\text{Sr}/^{86}\text{Sr}$ ratio over a geological time scale. As a result of the above-mentioned processes, the $^{87}\text{Sr}/^{86}\text{Sr}$ ratios nowadays measured in rock materials cover a wide range, depending upon the local geology, varying from ~ 0.703 in the depleted mantle, which is characterized by a low Rb/Sr ratio, to >0.900 in Archean granite and metasediments from the old continental crust.^{7–9}

During soil formation processes, minerals release Sr into the soil through mechanisms of differential weathering. Because each mineral is characterized by a specific $^{87}\text{Sr}/^{86}\text{Sr}$ ratio and Sr weather rate, the $^{87}\text{Sr}/^{86}\text{Sr}$ ratio of the bulk soil represents a

weighted average value of the bedrock.^{10,11} The soil isotope composition can also be affected by additional Sr sources, such as atmospheric depositions, irrigation, organic matter restitution, and other anthropogenic sources.^{12–16} Only a fraction of the total Sr present in the bulk soil is actually bioavailable for plant uptake. Although Sr is not an essential element, it is assumed that its uptake and internal transport follow the same pathway of calcium (Ca) because their properties are similar (e.g., ionic radius and valence), to the point that Sr is often used as a proxy to trace Ca within the tree.^{17–19} Similar to Ca, it is assumed that Sr ions are absorbed mainly from the upper soil horizons through the apical part of fine roots, where no Casparian band is present, and then transferred to the different plant organs mostly through the xylem sap.^{19–23} As a result of the low mass difference among isotopes, heavy elements, such as Sr, exhibit relatively little isotope fractionation (natural and instrumental) and mass bias can be mathematically corrected.^{17,24,25} Therefore, the corrected $^{87}\text{Sr}/^{86}\text{Sr}$ ratio of plants is closely related to that of the soil bioavailable fraction, ensuring a direct link with the growing environment and allowing for the use of the $^{87}\text{Sr}/^{86}\text{Sr}$ ratio as a traceability marker.^{5,17} Despite a lack of an official reference method to recover the soil bioavailable Sr, several authors obtained good correlation between the soil and plant $^{87}\text{Sr}/^{86}\text{Sr}$ ratio, extracting Sr from the soil with buffered solutions.^{19,26–29}

The geologic complexity and presence of multiple Sr inputs can undermine the strength of the correlation between the soil

Received: February 15, 2019

Revised: April 19, 2019

Accepted: April 23, 2019

Published: April 23, 2019

and plant $^{87}\text{Sr}/^{86}\text{Sr}$ ratio and, hence, this ratio in agricultural produces. For example, an unequal horizontal and vertical distribution of minerals in soils can lead to gradients of soil Sr isotope composition.¹⁰ To our knowledge, how the local Sr variability is reflected into changes of the $^{87}\text{Sr}/^{86}\text{Sr}$ ratio at the plant level has not yet been deeply investigated. Accounting for microscale variations of the $^{87}\text{Sr}/^{86}\text{Sr}$ ratio would greatly improve the prediction capability of models of the geographical distribution of Sr.

The aim of this study was to investigate the $^{87}\text{Sr}/^{86}\text{Sr}$ ratio variability at three levels, comparing subsamples of the same tree part (intrapart variability), different tree parts (intratree variability), and different trees of the same orchard (intertree variability). The $^{87}\text{Sr}/^{86}\text{Sr}$ ratio of tree samples was compared to their respective soil to verify if and to which extent the individual and spatial variability of the trees is linked to its soil heterogeneity.

MATERIALS AND METHODS

Reagents. Ammonium nitrate ($\geq 98\%$) was purchased from Sigma-Aldrich; cellulose acetate (CA) filters (0.45 μm) and polypropylene (PP) disposable vials were purchased from Vetrotecnica; and polytetrafluoroethylene (PTFE) filters (0.45 μm) were purchased from Thermo Fisher Scientific. Strontium separation was accomplished using a strontium-selective resin (Sr spec) purchased from TrisKem International. Monoelemental certified standards of rubidium (Rb) and strontium (Sr) were purchased from ULTRA Scientific; calcium (Ca) was purchased from Agilent Technologies; and scandium (Sc), germanium (Ge), and yttrium (Y) were purchased from Merck. Quality controls were prepared diluting the TMDA-54.5 certified reference material (LabService Analytica Srl) for inductively coupled plasma mass spectrometry (ICP-MS) and SRM 987 [National Institute of Standards and Technology (NIST)] with a certified Sr isotope composition for multicollector inductively coupled plasma mass spectrometry (MC ICP-MS). Nitric acid (65%, Merck) and high-purity deionized water (18.2 M Ω cm, Elix-Millipore), additionally purified through a sub-boiling duoPur distillation system (Milestone), were used throughout the entire experiment and analytical work. Vessels and vials were cleaned by an acid steam cleaning system (Trace Clean, Milestone). Reagents and chemicals were stored according to the instructions of the suppliers.

Sampling Sites. The study was conducted in two orchards located in two valleys of South Tyrol (North Italy). In each orchard, the study area was restricted to a block of adult apple trees (*Malus × domestica* Borkh., cultivar Gala, clone Schnitzer Schniga, rootstock M9). The distance between apple trees along the row is 0.8 m, and rows are 3 m apart. The apple orchards were cultivated following the recommendations of the South Tyrolean guidelines for integrated fruit production (www.agrios.it). The soil strip below the tree row (approximately 60 cm wide) was treated with non-residual herbicides to control weeds, while in the alleys, grasses were regularly mowed. One of the two orchards (orchard L), planted in 2010, is located in the Adige Valley, south of Bolzano, in the area of Laimburg [geographic coordinates, 46° 22' 48.0" N and 11° 17' 26.2" E; altitude, 226 m above sea level (asl); and area of the Gala block, ca. 16 500 m²]. Groundwater is used for drip irrigation. The soil has a silty-loamy texture (25% sand, 64% silt, and 11% clay), 2.7% of total organic carbon, a high content of carbonates, and a pH value in CaCl₂ equal to 7.7. The other orchard (orchard S), planted in 2007, is located in Val Venosta, close to the village of Sluderno (geographic coordinates, 46° 39' 24.7" N and 10° 34' 37.1" E; altitude, 900 m asl; and area of the Gala block, ca. 700 m²). Groundwater is used for overhead sprinkler irrigation. The soil has a loamy texture (44% sand, 44% silt, and 12% clay), 4.3% of total organic carbon, low carbonate content, and a pH value in CaCl₂ equal to 5.9. Geologically, the two sites are located in areas characterized by recent alluvial deposits.³⁰ Moreover, it is documented that, between 1930 and 1940, the orchard of Sluderno was backfilled with soil from a lateral valley.

Sampling Campaign. At fruit harvest (August–September 2016), six apple trees were randomly selected in both orchards (Figure S1 of the Supporting Information). Two of the six trees were adjacent to each other within the same row. From each tree, six shoots (shoot axes with their leaves) and six fruits were collected at 1–2 m of height from the ground from different tree branches. All of the subsamples were kept separated and not pooled in a bulk sample. The soil was sampled from three different points around each tree, at ca. 30 cm from the tree trunk base (within the projection area of the canopy of the tree). When the soil around the two adjacent trees was collected, the sampling was carried out in the weeded area between the two trees at 20 and 40 cm of distance from the tree trunks, respectively. Soil cores were collected from the layer between 10 and 20 cm depth with a soil core sampler (5 cm in diameter).²⁶ All of the soil samples were processed and analyzed separately.

In May 2017, a second soil sampling was performed to a depth of 80 cm between three randomly selected pairs of adjacent trees per orchard, in an area equidistant from the trees. After the first 10 cm was discharged, the soil core was divided into subsets of 10 cm each. From the two adjacent trees, 10 leaves each were randomly collected and then pooled to obtain a bulk sample to compare to the soil Sr isotope profile along the soil. All of the soil subfractions of each soil core were processed and analyzed separately.

Sample Preparation. Sr Extraction from Soil Samples. Soil samples were sieved at 2 mm, and all of the root pieces were manually picked out. Samples were dried at 40 °C for 48 h. The Sr-bioavailable fraction was extracted according to the official method DIN ISO 19730,³¹ in agreement with other authors,^{3,26} and then filtered with CA filters (0.45 μm).

Acid Digestion of Vegetable Samples. For each tree part (shoot axes, leaves, and apples subsequently divided in peel and pulp), all of the six subsamples were processed and analyzed separately. Samples were repeatedly washed with distilled water to remove dust and deposits from their surface. Leaves with their petiole were manually separated from their shoot axis, and both the organs were oven-dried at 65 °C for 48 h. The apple peel was manually separated from the pulp with a peeler. Then, the central disk of the pulp (ca. 1 cm thickness) was cut and deprived of the fruit core. The peel and pulp central disk were freeze-dried in a FreeZone apparatus (Labconco). Once all samples were powdered, 0.5 g of each sample was digested with 5 mL of HNO₃ (65%, w/w) in a Milestone UltraWAVE apparatus.¹⁵ Digested samples were filtered with PTFE filters (0.45 μm), transferred into vials, and filled to 10 mL with distilled water.

Sr/Matrix Separation. To eliminate elements that can interfere with analysis, especially Ca and Rb, a manual separation of Sr was performed with a Sr-specific resin (Triskem International), according to the method proposed by Swoboda et al.,³ with slight modifications. The separation procedure followed these steps: (i) resin activation with 5.5 mL of 8 M HNO₃, (ii) sample load (8 M HNO₃), (iii) washing with 8 M HNO₃ (the volume of the acid solution during the washing step was 3.5 mL for leaves and branches and 4.5 mL for soil and apple pulp and peel), and (iv) Sr recovery with 8 mL of distilled water. After the effective Sr/matrix separation was verified at ICP-MS, the final concentration of the Sr solutions was adjusted to 200 ng/g, except for apple peel and pulp samples, for which it was adjusted to 20 ng/g.

ICP-MS and MC ICP-MS Analyses. The quantitative analysis of Ca, Rb, and Sr was performed through an inductively coupled plasma mass spectrometer (iCAP Q ICP-MS, Thermo Scientific, Bremen, Germany) equipped with an autosampler ASX-520 (Cetac Technologies, Inc., Omaha, NE, U.S.A.). The calibration curve was prepared diluting a stock solution of standards to reach the range of 0.1–250 ng/g for Rb and Sr and 0.01–50 $\mu\text{g/g}$ for Ca. Instrumental blanks were also included. A standard solution of Sc, Ge, and Y was used as the internal standard. Instrumental accuracy was evaluated measuring the certified reference material TMDA-64.3 and was on average always comprised between 90 and 110%.

$^{87}\text{Sr}/^{86}\text{Sr}$ was measured with a double-focusing multicollector inductively coupled plasma mass spectrometer (Neptune Plus, Thermo Scientific, Bremen, Germany) with a forward Nier–Johnson

Table 1. Concentrations of Ca, Rb, and Sr and Ca/Sr Molar Ratio in the Different Tree Parts for the Two Orchards^a

orchard	tree part	Ca ($\mu\text{g/g}$)	Rb ($\mu\text{g/g}$)	Sr ($\mu\text{g/g}$)	Ca/Sr (mmol/ μmol)
L	shoot axis	17588 \pm 6105	3.8 \pm 1.8	64.7 \pm 19.0	0.60 \pm 0.14
	leaf	21815 \pm 7275	7.3 \pm 3.5	67.8 \pm 26.9	0.74 \pm 0.15
	apple peel	806 \pm 239	3.9 \pm 1.5	1.2 \pm 0.5	1.53 \pm 0.29
	apple pulp	319 \pm 84	5.1 \pm 1.9	1.1 \pm 0.3	0.63 \pm 0.10
S	shoot axis	17940 \pm 4978	10.6 \pm 6.2	59.3 \pm 16.7	0.67 \pm 0.06
	leaf	16131 \pm 3935	19.3 \pm 13.5	42.6 \pm 12.0	0.84 \pm 0.09
	apple peel	905 \pm 192	11.7 \pm 7.8	1.2 \pm 0.3	1.66 \pm 0.20
	apple pulp	374 \pm 77	15.0 \pm 9.7	1.2 \pm 0.3	0.72 \pm 0.10

^aFor each tree part, the mean \pm sd of 36 samples is reported.

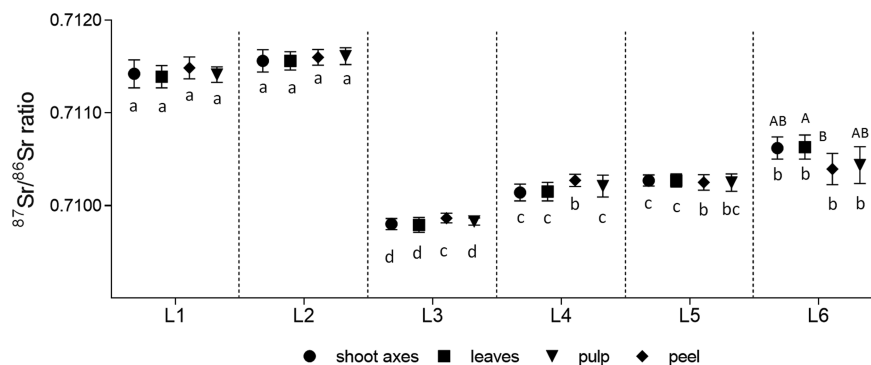


Figure 1. $^{87}\text{Sr}/^{86}\text{Sr}$ ratio measured in different organs/tissues of the six apple trees sampled in orchard L. Each point represents the mean \pm sd of six samples. Lowercase letters identify significant differences for the same tissue among different trees, and capital letters identify significant differences for different organs/tissues within the same tree. When letters are not present, differences are not significant.

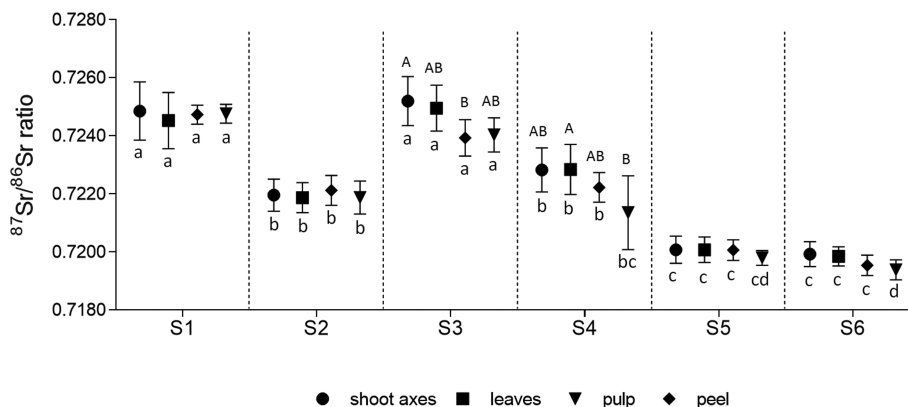


Figure 2. $^{87}\text{Sr}/^{86}\text{Sr}$ ratio measured in different organs/tissues of the six apple trees sampled in orchard S. Each point represents the mean \pm sd of six samples. Lowercase letters identify significant differences for the same tissue among different trees, and capital letters identify significant differences for different organs/tissues within the same tree. When letters are not present, differences are not significant.

geometry. A Ni sampler and skimmer cone were used. The analysis was carried out in static mode and low resolution. The multicollector was equipped with nine Faraday cups, eight of which are moveable and one fixed (configuration: L4, ^{82}Kr ; L3, ^{83}Kr ; L2, ^{84}Sr , L1, ^{85}Rb ; C, ^{86}Sr ; H1, ^{87}Sr ; and H2, ^{88}Sr) and $10^{11} \Omega$ resistors as amplifiers. The instrument was tuned daily, and its accuracy was determined analyzing the NIST SRM 987 certified reference solution at the beginning, at the end, and at every block of samples in the sequence,^{1,32} bracketed with a blank solution. Replicated measurements of SRM 987 provided an average ratio of 0.710247 ± 0.000013 (the uncertainty is expressed as twice the standard deviation) within the measuring period of this study, consistent with both the certified value (0.71034 ± 0.00026) and “generally accepted” value [0.71026 ± 0.00002 , with the uncertainty expressed as twice the standard deviation (sd)].

Raw data were corrected as follows: blank subtraction, mass bias correction normalizing the $^{88}\text{Sr}/^{86}\text{Sr}$ value to the International Union

of Pure and Applied Chemistry (IUPAC) value of 8.3752,³³ and mathematical correction for the isobaric interference of ^{86}Kr and ^{87}Rb .²⁶ Soil, shoot axis, and leaf samples were measured in wet plasma conditions, while apple peel and pulp samples were measured in dry-plasma conditions (CETAC Aridus apparatus as the aerosol drying unit and jet sample cone + H Ni skimmer cone).

All of the analyzed solutions at ICP-MS and MC ICP-MS were adjusted to reach a final concentration of 2% nitric acid. Instrumental conditions were reported in a previous study.¹⁵

Statistical Analysis. First, the $^{87}\text{Sr}/^{86}\text{Sr}$ ratio of apple tree organs and tissues were analyzed on three levels. The intrapart variability was evaluated comparing the dispersion (sd) of the $^{87}\text{Sr}/^{86}\text{Sr}$ ratio around the mean value for the subsamples of each tree part. The analysis of variance (ANOVA) was performed first to compare the $^{87}\text{Sr}/^{86}\text{Sr}$ ratio among different tree parts within each tree (intrapart variability) and then to evaluate the variability of the $^{87}\text{Sr}/^{86}\text{Sr}$ ratio among the trees (intertree variability). The post hoc Tukey honest significant

difference (HSD) test at a 5% level of probability was used for pairwise comparisons. A two-tailed t test for paired samples was applied to compare the average $^{87}\text{Sr}/^{86}\text{Sr}$ ratio of the tree leaves to the soil at 10–20 cm for the first sampling. Moreover, the t test was performed to verify differences between leaf and soil samples measured at the two samplings. The level of significance was fixed at a p value of 0.05. A *priori* power analysis was performed to calculate the sample size in a simulated experimental design, taking this study as the reference pilot study, given the following parameters: p value, power ($1 - \beta$, with β equal to the probability of type II error), and effect size [difference between two means ($m_1 - m_2$) divided by the pooled sd].³⁴ Three different levels of effect size were used (0.8, 0.5, and 0.2), according to the classification of Sawilowsky.³⁵ The p value was set to 0.05, and power was set to 0.8. All of the statistical analyses were performed using the computing environment R (R Core Team).

RESULTS AND DISCUSSION

Intra- and Intertree Variability. Table 1 summarizes the average concentrations of Ca, Rb, and Sr found in the analyzed tree parts. Both Ca and Sr concentrations in leaves and in shoot axes were higher than in fruits.³⁶ The same allocation pattern of the two elements supports the use of Sr as a proxy for Ca.¹⁰ The Ca/Sr ratio (molar ratio) was similar for shoot axes, leaves, and apple pulp, while the apple peel showed higher ratios, in agreement with data from Živković et al.,³⁷ and might be due to the use of Ca solution as a spray treatment to reduce low-calcium physiological disorders in apples, such as cork spots and bitter pit. Ca from sprays, in fact, tends to accumulate in the peel and in the external cells of the pulp. Leaves and shoots also intercept and absorb Ca from sprays, but such amounts hardly modify the Ca concentration, which is already high.

Figures 1 and 2 report the $^{87}\text{Sr}/^{86}\text{Sr}$ ratio of the six subsamples for each tree part (organs and tissues) measured in the two orchards. In orchard L, the $^{87}\text{Sr}/^{86}\text{Sr}$ ratio ranged from 0.709 70 to 0.711 73 ($\Delta = 0.002 03$). The ratios measured in orchard S were between 0.718 95 and 0.725 98 ($\Delta = 0.007 03$), indicating a relatively higher content of radiogenic Sr than in orchard L. The average isotope ratio for the two orchards, calculated as the mean of each tree $^{87}\text{Sr}/^{86}\text{Sr}$ ratio, was $0.710 63 \pm 0.000 71$ (mean \pm sd) for orchard L and $0.722 19 \pm 0.002 14$ for orchard S. The $^{87}\text{Sr}/^{86}\text{Sr}$ ratios measured in the trees from orchard S covered a higher range than those measured in orchard L (Figures 1 and 2). This is not justified by the orchard area, because the sampled block of Gala trees in orchard S was much smaller than that in orchard L (Figure S1 of the Supporting Information).

Considering the average $^{87}\text{Sr}/^{86}\text{Sr}$ ratio dispersion for each tree part, the sd values of the six subsamples were on average lower for orchard L than for orchard S, 0.000 13 and 0.000 58, respectively (Figures 1 and 2). This lack of uniformity among subsamples and, hence, among different tree branches might reflect the fact that Sr, like Ca, is rather immobile within a plant and, once translocated from the absorbing roots to the leaves, is not remobilized and redistributed within the entire canopy.²¹ It is also likely that Sr transport within apple trees from the roots to the canopy follows a sectorial pattern instead of an integrated pattern, as highlighted for other nutrients,^{38–40} but additional studies would be required to support this point.

For both orchards, the ANOVA showed intratree homogeneity, indicated by no significant intratree differences among organs/tissues (Figures 1 and 2). The intratree homogeneity can also be appreciated in Figure 3, where the leaf ratios were plotted against those of their shoot axes, showing a high

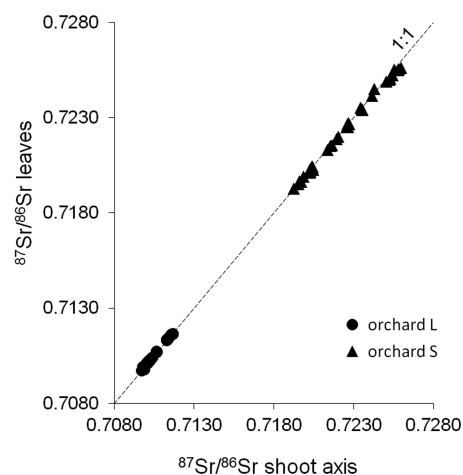


Figure 3. $^{87}\text{Sr}/^{86}\text{Sr}$ ratio of the leaves plotted against the $^{87}\text{Sr}/^{86}\text{Sr}$ ratio of the shoot axis where they were attached. Each point represents a subsample ($n = 36$).

correlation between the two organs, with R higher than 0.99, and a slope close to 1 for both of the orchards. Similar relationships were also obtained comparing the other organs/tissues (data not shown). The intertree homogeneity was rather low ($p < 0.001$) in both orchards, as it appears from the comparison of the $^{87}\text{Sr}/^{86}\text{Sr}$ ratio for the same tree part among the six trees sampled in each orchard (Figures 1 and 2). Generally, the same intertree trends were present in all of the organs/tissues, as determined through pairwise comparisons. Despite the overall lack of homogeneity, the two adjacent trees had the same isotopic composition in both of the orchards (L1 and L2 in Figure 1 and S5 and S6 in Figure 2). To better explain the intrapart variability and the intertree heterogeneity, the plant–soil relation was investigated.

Soil as a Source of Variability. The soil samples collected at a depth of 10–20 cm in orchard L had a Sr isotope ratio between 0.708 53 and 0.710 98, while the range was between 0.714 24 and 0.718 04 in orchard S (Table 2). The sd of the $^{87}\text{Sr}/^{86}\text{Sr}$ ratio in the soil samples collected below each tree, deriving from the independent analysis of the three soil subsamples, indicates a greater variability in orchard S than in orchard L (0.000 94 and 0.000 27, respectively). These results confirm the complexity of the soil matrix, showing that, even within a small area and at the same depth, there could be a relatively large variability of the $^{87}\text{Sr}/^{86}\text{Sr}$ ratio.

In Figure 4, the average $^{87}\text{Sr}/^{86}\text{Sr}$ ratio of the leaves of each single tree was plotted against the ratio in the soil collected close to the tree. While we found a good correlation between the two sets of data for orchard L ($R > 0.95$; Figure 4B), there was no correlation in orchard S (Figure 4). In light of the obtained results, we concluded that the intertree heterogeneity for orchard L is due to the heterogeneity of the soil $^{87}\text{Sr}/^{86}\text{Sr}$ ratio underneath each tree. Moreover, the variability of the $^{87}\text{Sr}/^{86}\text{Sr}$ ratio among the three soil sampling points at the same depth (10–20 cm) underneath each tree can also explain the intrapart variability: apple tree roots are, in fact, spread in the soil in different directions, and they absorb bioavailable Sr from the adjacent soil. If there is a horizontal variability of the $^{87}\text{Sr}/^{86}\text{Sr}$ ratio in the area surrounding the root system, this variability is then transferred to the tree canopy.

More detailed information about the $^{87}\text{Sr}/^{86}\text{Sr}$ ratio variability within the orchards was inferred from the results

Table 2. Results of the $^{87}\text{Sr}/^{86}\text{Sr}$ Ratio Analysis of Soil Samples Collected at 10–20 cm Depth^a

orchard	tree ID	L1/L2	L3	L4	L5	L6	mean per orchard	sd per orchard
L	mean per tree	0.71078	0.70928	0.70914	0.70968	0.71003	0.70978	0.00066
	sd per tree	0.00027	0.00018	0.00053	0.00016	0.00023		0.00027
orchard	tree ID	S1	S2	S3	S4	S5/S6	mean per orchard	sd per orchard
S	mean per tree	0.71546	0.71500	0.71622	0.71699	0.71560	0.71586	0.00077
	sd per tree	0.00094	0.00069	0.00158	0.00032	0.00119		0.00094

^aEach value per tree derives from the mean of the three soil subsamples collected beneath each tree.

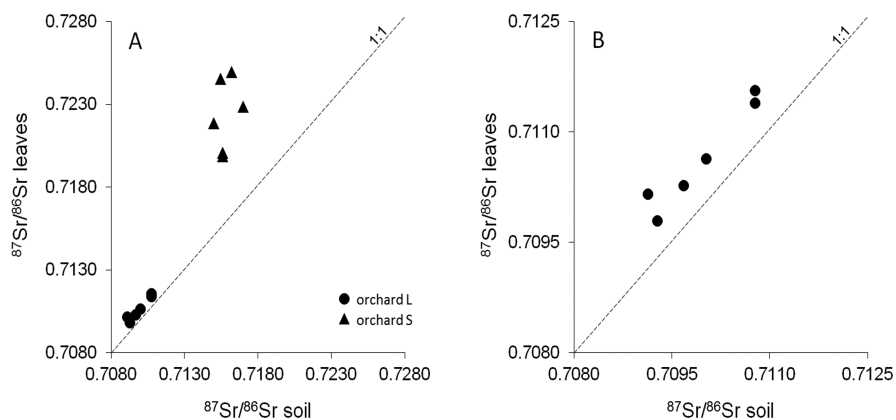


Figure 4. (A) $^{87}\text{Sr}/^{86}\text{Sr}$ ratio of the tree leaves plotted against the $^{87}\text{Sr}/^{86}\text{Sr}$ ratio of the soil collected close to the same tree at a depth of 10–20 cm. Average ratios for both orchards are represented ($n = 12$). (B) Data regarding orchard L are enlarged.

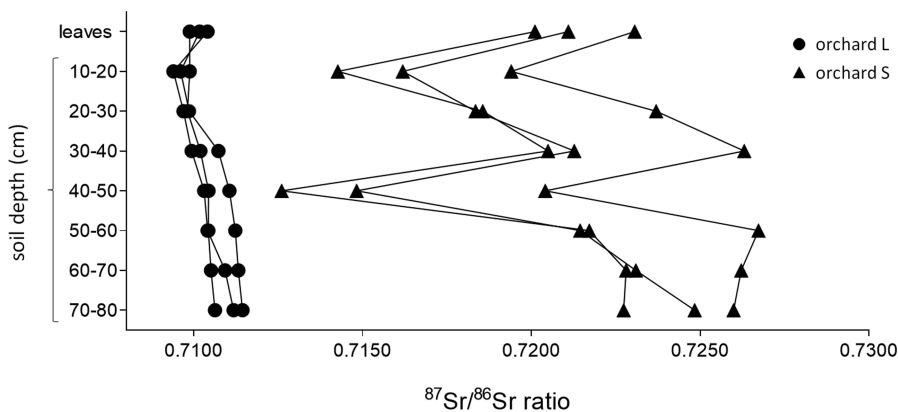


Figure 5. Leaf $^{87}\text{Sr}/^{86}\text{Sr}$ ratio plotted together with the corresponding $^{87}\text{Sr}/^{86}\text{Sr}$ profile in the soil. Each line connects values coming from the same sampling point.

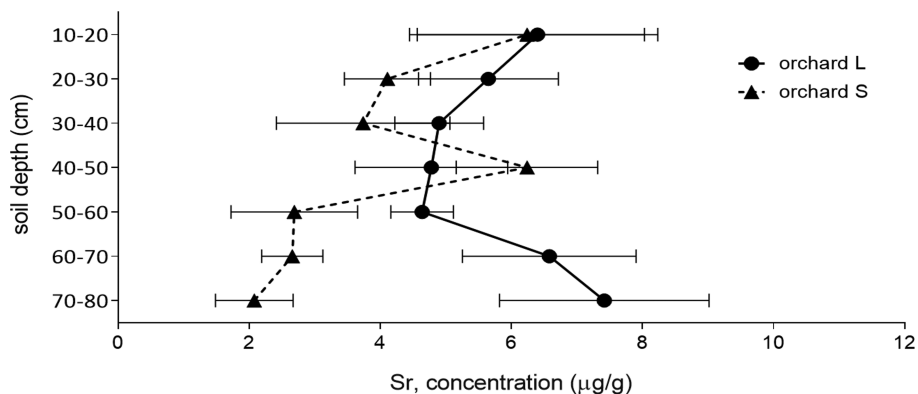


Figure 6. Sr concentration gradient along the soil profile (10–80 cm depth) for the three sampling sites within each orchard. Each point is the mean of the Sr concentration in the three soil cores at a specific depth.

Table 3. Results of the Power Analysis for Three Levels of Effect Size: Large (0.8), Medium (0.5), and Small (0.2)^a

n	effect size	large variability		small variability		small/large variability	
		pooled sd	$ m_1 - m_2 $	pooled sd	$ m_1 - m_2 $	pooled sd	$ m_1 - m_2 $
26	0.8	0.00206	0.00165	0.00066	0.00053	0.00153	0.00122
64	0.5	0.00206	0.00103	0.00066	0.00033	0.00153	0.00076
393	0.2	0.00206	0.00041	0.00066	0.00013	0.00153	0.00031

^aPower and *p* value were set at 0.8 and 0.05, respectively.

of the second sampling campaign (Figure 5). Moving from the shallower to the deeper layers, there was a slight increasing ⁸⁷Sr/⁸⁶Sr ratio in orchard L, while in orchard S, the variability among layers was rather high. In orchard S, the ratio raised from 0.716 62 to 0.722 69 moving from 10 to 40 cm, but in the 40–50 cm layer, there was an abrupt change of the ratio, with a value similar to that of the top layer (0.715 94). Then, the ratio increased again toward the deepest layers (Figure 5). The ratios measured in the layer between 10 and 20 cm during the first sampling (0.715 81 ± 0.001 11) fell within the range of values measured at the same layer during this sampling (0.716 62 ± 0.002 59), with no significant differences between the mean at the two sampling times. Inflection points, such as those found in the soil of orchard S, and differences in the ⁸⁷Sr/⁸⁶Sr profile of the soil comparing the results of multiple soil cores collected within the same area are quite common.^{26,41} Such a behavior depends upon the mineral composition of the soil and soil evolution that cause the release of Sr from minerals at different weathering rates through the geological eras.^{10,17,42} Factors such as climate, topography, and vegetation influence the soil formation processes and their rates.¹¹ Moreover, the topsoil is especially affected by secondary Sr sources or soil perturbations.⁴³ In orchard S, also the backfill that occurred in the past may have contributed to the overall heterogeneity of the soil layers, even though too little information about the backfill is available to properly reconstruct the event.

The samples collected from the tree canopies showed an average Sr isotope ratio of 0.710 35 ± 0.000 16 for orchard L and 0.721 42 ± 0.001 50 for orchard S (Figure 5), similar to those measured the previous year. In orchard S, we speculate that root Sr uptake was rather limited from the 40–50 cm soil layer: in fact, the Sr concentration (Figure 6) was especially high in the 40–50 cm layer (6.24 ± 1.08), but the ⁸⁷Sr/⁸⁶Sr ratio was low (0.715 94 ± 0.004 02).

Implications for Traceability Studies. In this study, we demonstrated that the variability of the soil Sr isotope ratio within an apple orchard can be significantly high within a restricted area, as in the case of orchard S, or rather limited in a much larger area, as in the case of orchard L. In addition, we also always observed that both the intrapart and the intertree variability of the ⁸⁷Sr/⁸⁶Sr ratio were related to the ⁸⁷Sr/⁸⁶Sr variability in the soil. A high intratree homogeneity emerged comparing different tree parts (shoot axes, leaves, apple peels, and pulps). In the perspective of traceability studies based on the ⁸⁷Sr/⁸⁶Sr ratio, this result implies that the sampling can be performed indifferently in one of the tree parts, without significantly affecting the measured ratios. This aspect is of great importance, especially considering that fruits and, more in general, horticultural products are only seasonally available.

The requisites to apply the Sr isotope ratio method in traceability studies rely on the assumption that this ratio is mineral-dependent; therefore, it varies according to the local

geological features. In relation to the variability of the ⁸⁷Sr/⁸⁶Sr ratio, geological complexity plays a pivotal role. The ⁸⁷Sr/⁸⁶Sr ratio shows a low variability in geologically simple areas (e.g., ancient ocean basins), while it has rather high variability in complex regions (e.g., mountainous areas and accretionary terranes).¹¹ This complexity can lead to a large range of isotopic composition within a limited area, as reported in the literature,^{44,45} and it entails difficulties in determining if the sample size is representative for the explored area. When the intraregion variability of the ⁸⁷Sr/⁸⁶Sr ratio is high, it more likely overlaps with the values of other regions. Consequently, given a certain sample size, a decrease in the classification power of the ⁸⁷Sr/⁸⁶Sr ratio according to the product origin may occur, limiting the possibility to predict the origin of unknown samples in traceability and authenticity studies.

To better clarify this point, we performed power analysis, taking this investigation as a pilot study, to define the proper sample size per orchard for further studies. Considering the two orchards of this study, the effect size (*d*) was huge according to the classification of Sawilowsky [*d* (0.01), very small; *d* (0.2), small; *d* (0.5), medium; *d* (0.8), large; *d* (1.2), very large; and *d* (2.0), huge].³⁵ Therefore, our sample size was acceptable to detect a significant difference between the ⁸⁷Sr/⁸⁶Sr ratios of the two orchards. However, if the effect size decreased to 0.8, 0.5, or 0.2, the calculated sample size would dramatically increase to 26, 64, or 393, respectively (Table 3). For each effect size, we calculated what should be the minimum difference between the mean ⁸⁷Sr/⁸⁶Sr ratio of two orchards ($|m_1 - m_2|$) when both of them show large or small sd. In the first case, we simulated that both orchards had the sd of orchard S, while in the second case, we simulated that both orchards had the sd of orchard L. From our results (Table 3), considering a large effect size (0.8), the calculated $|m_1 - m_2|$ is 0.001 65 and 0.000 53, respectively. Finally, we evaluated the case of orchards with small/large sd, as in this study, obtaining a calculated $|m_1 - m_2|$ with a large effect size equal to 0.001 22, lower than what we actually found.

Another implication emerging from these results regards the possibility to generalize the measured data over a large area or other species.^{45,46} To create a reliable and comprehensive data set of Sr isotope ratios for samples with known origin, the sampling campaign should be adequately planned to collect representative samples and to guarantee an extensive sampling coverage, especially for the areas characterized by a high local to regional geologic complexity. However, this planning is not easily accomplished because it requires interdisciplinary knowledge of the area or the possibility to perform preliminary studies. Local heterogeneity also increases the difficulty of developing accurate predictive models. Indeed, high intra-area variability can lead to a consistent number of under- or overpredicted empirical data that significantly differ from the true value, especially if the model combines results from samples of different nature, as described by other authors.¹¹ When species characterized by different root growth along the

soil profile are grown in an area characterized by high geological complexity, they might differ in their Sr isotope composition, because bioavailable Sr is absorbed from different layers.

In conclusion, this study highlighted that different organs sampled from the same part of the canopy have a rather homogeneous $^{87}\text{Sr}/^{86}\text{Sr}$ ratio, while the same organ collected from different branches of the same trees might slightly differ in the isotopic ratio. Different trees from the same orchard might show some variability of the $^{87}\text{Sr}/^{86}\text{Sr}$ ratio, whose extent depends upon the horizontal and vertical variability in the soil $^{87}\text{Sr}/^{86}\text{Sr}$ ratio. For such a reason, the size of sampling must be planned carefully.

■ ASSOCIATED CONTENT

● Supporting Information

The Supporting Information is available free of charge on the ACS Publications website at DOI: [10.1021/acs.jafc.9b01082](https://doi.org/10.1021/acs.jafc.9b01082).

Orthophoto of orchards of (A) L and (B) S with sampling point distribution (Figure S1) (PDF)

■ AUTHOR INFORMATION

Corresponding Author

*E-mail: agnese.aguzzoni@unibz.it.

ORCID

Agnese Aguzzoni: [0000-0001-9001-1659](https://orcid.org/0000-0001-9001-1659)

Author Contributions

†Agnese Aguzzoni and Michele Bassi contributed equally as main authors to the presented work.

Funding

The Autonomous Province of Bozen-Bolzano, Department of Innovation, Research and University is gratefully acknowledged for its financial support within the NOI Capacity Building I Funding Frame (Decision 1472, 07.10.2013) and Capacity Building II Funding Frame (Decision 864, 04.09.2018). The authors thank the Department of Innovation, Research and University of the Autonomous Province of Bozen/Bolzano for covering the Open Access publication costs. The Laimburg Research Centre is funded by the Autonomous Province of Bozen-Bolzano.

Notes

The authors declare no competing financial interest.

■ REFERENCES

- (1) Hiraoka, H.; Morita, S.; Izawa, A.; Aoyama, K.; Shin, K.-C.; Nakano, T. Tracing the geographical origin of onions by strontium isotope ratio and strontium content. *Anal. Sci.* **2016**, *32* (7), 781–788.
- (2) Trincerini, P. R.; Baffi, C.; Barbero, P.; Pizzoglio, E.; Spalla, S. Precise determination of strontium isotope ratios by TIMS to authenticate tomato geographical origin. *Food Chem.* **2014**, *145*, 349–355.
- (3) Swoboda, S.; Brunner, M.; Boulyga, S. F.; Galler, P.; Horacek, M.; Prohaska, T. Identification of Marchfeld asparagus using Sr isotope ratio measurements by MC-ICP-MS. *Anal. Bioanal. Chem.* **2008**, *390*, 487–494.
- (4) Aoyama, K.; Nakano, T.; Shin, K.-C.; Izawa, A.; Morita, S. Variation of strontium stable isotope ratios and origins of strontium in Japanese vegetables and comparison with Chinese vegetables. *Food Chem.* **2017**, *237*, 1186–1195.
- (5) Baffi, C.; Trincerini, P. R. Food traceability using the $^{87}\text{Sr}/^{86}\text{Sr}$ isotopic ratio mass spectrometry. *Eur. Food Res. Technol.* **2016**, *242* (9), 1411–1439.
- (6) Faure, G.; Powell, J. L. The Geochemistry of Rubidium and Strontium. *Strontium Isotope Geology*; Springer: Berlin, Germany, 1972; Minerals, Rocks and Inorganic Materials (Monograph Series of Theoretical and Experimental Studies), Vol. 5, pp 1–8, DOI: [10.1007/978-3-642-65367-4_1](https://doi.org/10.1007/978-3-642-65367-4_1).
- (7) Banner, J. L. Radiogenic isotopes: Systematics and applications to earth surface processes and chemical stratigraphy. *Earth-Sci. Rev.* **2004**, *65* (3–4), 141–194.
- (8) Jacobsen, S. B.; Dymek, R. F. Nd and Sr isotope systematics of clastic metasediments from Isua, West Greenland: Identification of pre-3.8 Ga Differentiated Crustal Components. *J. Geophys. Res. Solid Earth* **1988**, *93* (B1), 338–354.
- (9) Sillen, A.; Hall, G.; Richardson, S.; Armstrong, R. $^{87}\text{Sr}/^{86}\text{Sr}$ ratios in modern and fossil food-webs of the Sterkfontein Valley: Implications for early hominid habitat preference. *Geochim. Cosmochim. Acta* **1998**, *62* (14), 2463–2473.
- (10) Drouet, T.; Herbauts, J.; Gruber, W.; Demaiffe, D. Natural strontium isotope composition as a tracer of weathering patterns and of exchangeable calcium sources in acid leached soils developed on loess of central Belgium. *Eur. J. Soil Sci.* **2007**, *58* (1), 302–319.
- (11) Crowley, B. E.; Miller, J. H.; Bataille, C. P. Strontium isotopes ($^{87}\text{Sr}/^{86}\text{Sr}$) in terrestrial ecological and palaeoecological research: Empirical efforts and recent advances in continental-scale models. *Biol. Rev.* **2017**, *92* (1), 43–59.
- (12) Hartman, G.; Richards, M. Mapping and defining sources of variability in bioavailable strontium isotope ratios in the Eastern Mediterranean. *Geochim. Cosmochim. Acta* **2014**, *126*, 250–264.
- (13) Techer, I.; Lancelot, J.; Descroix, F.; Guyot, B. About Sr isotopes in coffee 'Bourbon Pointu' of the Réunion Island. *Food Chem.* **2011**, *126* (2), 718–724.
- (14) Maurer, A.-F.; Galer, S. J. G.; Knipper, C.; Beierlein, L.; Nunn, E. V.; Peters, D.; Tütken, T.; Alt, K. W.; Schöne, B. R. Bioavailable $^{87}\text{Sr}/^{86}\text{Sr}$ in different environmental samples — Effects of anthropogenic contamination and implications for isoscapes in past migration studies. *Sci. Total Environ.* **2012**, *433*, 216–229.
- (15) Aguzzoni, A.; Bassi, M.; Robatscher, P.; Tagliavini, M.; Tirlir, W.; Scandellari, F. Plant Sr isotope ratios as affected by the Sr isotope ratio of the soil and of the external Sr inputs. *J. Agric. Food Chem.* **2018**, *66* (40), 10513–10521.
- (16) Stewart, B. W.; Capo, R. C.; Chadwick, O. A. Quantitative strontium isotope models for weathering, pedogenesis and biogeochemical cycling. *Geoderma* **1998**, *82* (1–3), 173–195.
- (17) Capo, R. C.; Stewart, B. W.; Chadwick, O. A. Strontium isotopes as tracers of ecosystem processes: Theory and methods. *Geoderma* **1998**, *82* (1–3), 197–225.
- (18) Kabata-Pendias, A. *Trace Elements in Soils and Plants*, 4th ed.; CRC Press: Boca Raton, FL, 2011.
- (19) Blum, J. D.; Dasch, A. A.; Hamburg, S. P.; Yanai, R. D.; Arthur, M. A. Use of foliar Ca/Sr discrimination and $^{87}\text{Sr}/^{86}\text{Sr}$ ratios to determine soil Ca sources to sugar maple foliage in a northern hardwood forest. *Biogeochemistry* **2008**, *87* (3), 287–296.
- (20) Dambrine, E.; Loubet, M.; Vega, J. A.; Lissarague, A. Localisation of mineral uptake by roots using Sr isotopes. *Plant Soil* **1997**, *192* (1), 129–132.
- (21) Pandey, R. Mineral Nutrition of Plants. In *Plant Biology and Biotechnology*; Bahadur, B., Venkat Rajam, M., Sahijram, L., Krishnamurthy, K. V., Eds.; Springer: New Delhi, India, 2015; pp 499–538, DOI: [10.1007/978-81-322-2286-6_20](https://doi.org/10.1007/978-81-322-2286-6_20).
- (22) Schmitt, A.-D.; Gangloff, S.; Labolle, F.; Chabaux, F.; Stille, P. Calcium biogeochemical cycle at the beech tree-soil solution interface from the Strengbach CZO (NE France): Insights from stable Ca and radiogenic Sr isotopes. *Geochim. Cosmochim. Acta* **2017**, *213*, 91–109.
- (23) White, P. J.; Broadley, M. R. Calcium in plants. *Ann. Bot.* **2003**, *92* (4), 487–511.
- (24) Horsky, M.; Irrgeher, J.; Prohaska, T. Evaluation strategies and uncertainty calculation of isotope amount ratios measured by MC ICP-MS on the example of Sr. *Anal. Bioanal. Chem.* **2016**, *408* (2), 351–367.

- (25) Yang, L. Accurate and precise determination of isotopic ratios by MC-ICP-MS: A review. *Mass Spectrom. Rev.* **2009**, *28* (6), 990–1011.
- (26) Durante, C.; Baschieri, C.; Bertacchini, L.; Cocchi, M.; Sighinolfi, S.; Silvestri, M.; Marchetti, A. Geographical traceability based on $^{87}\text{Sr}/^{86}\text{Sr}$ indicator: A first approach for PDO Lambrusco wines from Modena. *Food Chem.* **2013**, *141* (3), 2779–2787.
- (27) Liu, H.; Wei, Y.; Lu, H.; Wei, S.; Jiang, T.; Zhang, Y.; Guo, B. Combination of the $^{87}\text{Sr}/^{86}\text{Sr}$ ratio and light stable isotopic values ($\delta^{13}\text{C}$, $\delta^{15}\text{N}$ and δD) for identifying the geographical origin of winter wheat in China. *Food Chem.* **2016**, *212*, 367–373.
- (28) Song, B.; Ryu, J.; Shin, H. S.; Lee, K. Determination of the source of bioavailable Sr using tracers: A case study of hot pepper and rice. *J. Agric. Food Chem.* **2014**, *62*, 9232–9238.
- (29) Poszwa, A.; Ferry, B.; Dambrine, E.; Pollier, B.; Wickman, T.; Loubet, M.; Bishop, K. Variations of bioavailable Sr concentration and $^{87}\text{Sr}/^{86}\text{Sr}$ ratio in boreal forest ecosystems: Role of biocycling, mineral weathering and depth of root uptake. *Biogeochemistry* **2004**, *67* (1), 1–20.
- (30) Istituto Superiore per la Protezione e la Ricerca Ambientale (ISPRA). *Carta Geologica d'Italia Scala 1:100.000*; http://193.206.192.231/carta_geologica_italia/nord.htm (accessed Oct 3, 2018).
- (31) Technical Committee ISO/TC 190 Subcommittee SC3. *Soil Quality—Extraction of Trace Elements from Soil Using Ammonium Nitrate Solution*; International Organization for Standardization (ISO): Geneva, Switzerland, 2008.
- (32) Lagad, R. A.; Singh, S. K.; Rai, V. K. Rare earth elements and $^{87}\text{Sr}/^{86}\text{Sr}$ isotopic characterization of Indian Basmati rice as potential tool for its geographical authenticity. *Food Chem.* **2017**, *217*, 254–265.
- (33) Meija, J.; Coplen, T. B.; Berglund, M.; Brand, W. A.; De Bièvre, P.; Gröning, M.; Holden, N. E.; Irrgeher, J.; Loss, R. D.; Walczyk, T.; Prohaska, T. IUPAC Technical Report Isotopic compositions of the elements 2013 (IUPAC Technical Report). *Pure Appl. Chem.* **2016**, *88* (3), 293–306.
- (34) Cohen, J. *Statistical Power Analysis for the Behavioral Sciences*; Lawrence Erlbaum Associates: Hillsdale, NJ, 1988.
- (35) Sawilowsky, S. S. New Effect Size Rules of Thumb. *J. Mod. Appl. Stat. Methods* **2009**, *8* (2), 597–599.
- (36) Zanotelli, D.; Rechenmacher, M.; Guerra, W.; Cassar, A.; Tagliavini, M. Seasonal Uptake Rate Dynamics and Partitioning of Mineral Nutrients by Bourse Shoots of Field-grown Apple Trees. *Eur. J. Hort. Sci.* **2014**, *79* (4), 203–211.
- (37) Živković, J.; Šavikin, K.; Zdunić, G.; Dojčinović, B.; Menković, N. Phenolic and mineral profile of Balkan indigenous apple and pear cultivars. *J. Serb. Chem. Soc.* **2016**, *81* (6), 607–621.
- (38) Orians, C. M.; Ardon, M.; Mohammad, B. A. Vascular architecture and patchy nutrient availability generate within-plant heterogeneity in plant traits important to herbivores. *Am. J. Bot.* **2002**, *89* (2), 270–278.
- (39) Orians, C. M.; van Vuuren, M. M. I.; Harris, N. L.; Babst, B. A.; Ellmore, G. S. Differential sectoriality in long-distance transport in temperate tree species: Evidence from dye flow, ^{15}N transport, and vessel element pitting. *Trees* **2004**, *18* (5), 501–509.
- (40) Price, E. A. C.; Hutchings, M. J.; Marshall, C. Causes and consequences of sectoriality in the clonal herb *Glechoma hederacea*. *Vegetatio* **1996**, *127* (1), 41–54.
- (41) Meek, K.; Derry, L.; Sparks, J.; Cathles, L. $^{87}\text{Sr}/^{86}\text{Sr}$, Ca/Sr, and Ge/Si ratios as tracers of solute sources and biogeochemical cycling at a temperate forested shale catchment, central Pennsylvania, USA. *Chem. Geol.* **2016**, *445*, 84–102.
- (42) Prunier, J.; Chabaux, F.; Stille, P.; Gangloff, S.; Pierret, M. C.; Viville, D.; Aubert, A. Geochemical and isotopic (Sr, U) monitoring of soil solutions from the Strengbach catchment (Vosges mountains, France): Evidence for recent weathering evolution. *Chem. Geol.* **2015**, *417*, 289–305.
- (43) Prohaska, T.; Wenzel, W. W. W.; Stinger, G. ICP-MS-based tracing of metal sources and mobility in a soil depth profile via the isotopic variation of Sr and Pb. *Int. J. Mass Spectrom.* **2005**, *242* (2–3), 243–250.
- (44) Blum, J. D.; Taliaferro, E. H.; Weisse, M. T.; Holmes, R. T. Changes in Sr/Ca, Ba/Ca and $^{87}\text{Sr}/^{86}\text{Sr}$ ratios between trophic levels in two forest ecosystems in the northeastern U.S.A. *Biogeochemistry* **2000**, *49* (1), 87–101.
- (45) Durante, C.; Bertacchini, L.; Cocchi, M.; Manzini, D.; Marchetti, A.; Rossi, M. C.; Sighinolfi, S.; Tassi, L. Development of $^{87}\text{Sr}/^{86}\text{Sr}$ maps as targeted strategy to support wine quality. *Food Chem.* **2018**, *255*, 139–146.
- (46) Brunner, M.; Katona, R.; Stefánka, Z.; Prohaska, T. Determination of the geographical origin of processed spice using multielement and isotopic pattern on the example of Szegedi paprika. *Eur. Food Res. Technol.* **2010**, *231* (4), 623–634.